IC-Processed Hot-Filament Vacuum Microdevices

Kirt R. Williams and Richard S. Muller
Berkeley Sensor & Actuator Center
An Industry/University/NSF Cooperative Research Center
Department of Electrical Engineering and Computer Sciences
University of California, Berkeley, CA 94720

Abstract

Micromachined vacuum devices that employ a hot tungsten filament as a source of electromagnetic radiation and thermionically emitted electrons have been fabricated. These hot-filament devices have been characterized for use as "microlamps," vacuum diodes, and triodes. Coplanar filaments are used for the cathodes and anodes in the diodes, and also for the grids in the triodes. The filaments are typically 200-μm long and are suspended over a cavity in the silicon substrate. The devices tested were operated in a pumped vacuum chamber.

Introduction

Hot-filament vacuum microdevices have been made using IC-fabrication techniques. Vacuum-emission devices have the advantage over their solid-state counterparts of operation with minimal degradation in high-temperature and high-radiation environments, and may also offer speed advantages.

Many researchers are studying high-electric-field vacuum microdevices, which typically use sharply pointed conical or wedge-shaped tips at room temperature as the cathodes [1]. In contrast, in this research we employ thermionic emission from heated tungsten filaments as the source of electrons in devices we call "microtubes." This approach has been used by other researchers using heated polysilicon filaments [2].

All of our microtubes have structures similar to that of the triode shown in Fig. 1. The coplanar filaments are made of tungsten and are typically 200 μm long, 3-15 μm wide, and 0.7 μm thick. They are suspended over a cavity etched into a silicon substrate, and are insulated from the substrate by layers of phosphosilicate glass and silicon nitride. During operation, the cathode filament is resistively heated by passing a large current through it (*not* indirectly heated as is usual in macroscopic vacuum tubes). Because the devices have not been carried through final cavity-sealing steps, they are operated in a pumped vacuum chamber at a pressure of about 10^{-4} Torr.

During operation of the microtube diodes and triodes, electrons flow horizontally from the cathode to the anode, in contrast to the vertical flow employed in most field-emission devices. An advantage of this horizontal structure is that as many electrodes as desired can be inserted between the cathode and anode to form triodes, tetrodes, and other multi-electrode devices. These more complicated devices can be

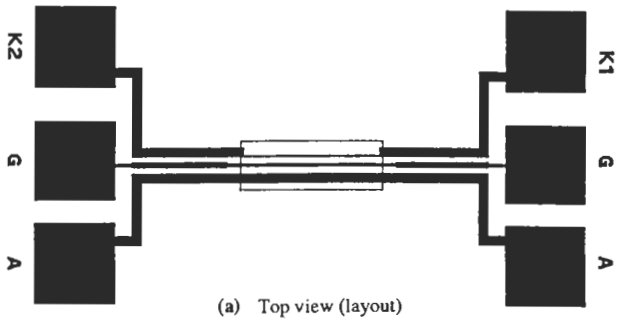

(a) Top view (layout)

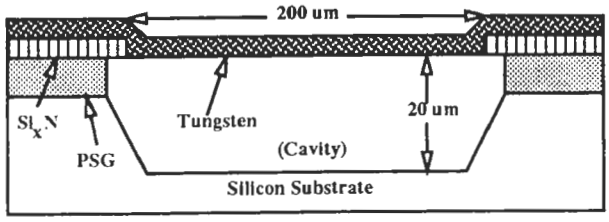

(b) Cross section along length of a filament (not to scale)

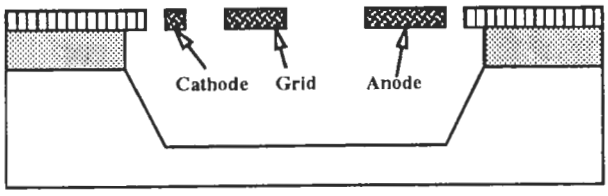

(c) Cross section across width of a filament (not to scale)

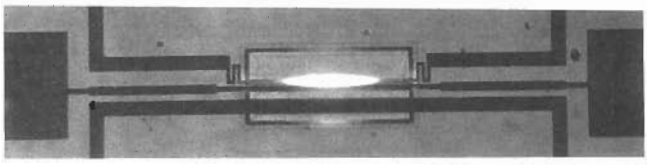

(d) Optical photograph with the cathode heated

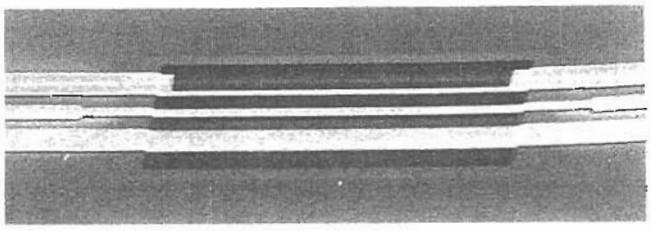

(e) SEM photograph

Fig. 1 A typical hot-filament vacuum device (triode shown here)

0-7803-0817-4/92 $3.00 © 1992 IEEE

designed to obtain desired operating characteristics (e.g. high small-signal output resistance), to perform complicated circuit functions (e.g. frequency mixing), or as sensors. The field patterns in the coplanar-electrode devices are, however, not optimal for triode or diode operation.

Because the cathode filament in these microtubes is heated to incandescence for thermionic emission (Fig. 1d), the device can also function as a microscopic broadband radiation source (microlamp), as has been previously demonstrated with a polysilicon filament sealed in vacuum cavity [3]. Due to their low melting point, however, polysilicon filaments can only emit relatively faint radiation that peaks in the infrared-to-red portion of the spectrum. With tungsten filaments, microlamps can be heated sufficiently to emit intense white light.

Fabrication

Device fabrication begins with ~20 Ω·cm *p*-type (100)-oriented silicon wafers. The wafers are coated with a 4-μm-thick sacrificial layer of low-pressure chemical-vapor deposited (LPCVD) phosphosilicate glass (PSG) and annealed at 1000°C for 1 hour. Next, 0.5 μm of silicon-rich LPCVD silicon nitride (Si_xN), which has a lower residual stress than that of stochiometric Si_3N_4, is deposited. The Si_xN is lithographically patterned and etched in an SF_6 + He plasma, leaving behind a rectangular window (Fig. 2a).

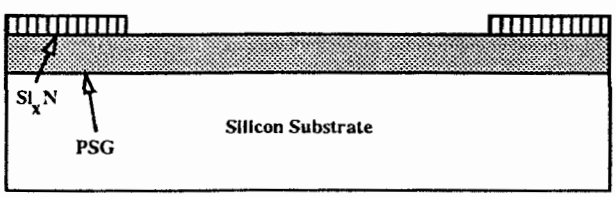

(a) After opening silicon nitride window

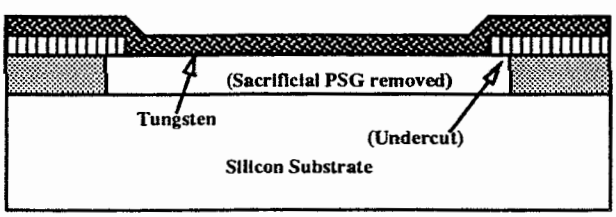

(b) After removing sacrificial PSG

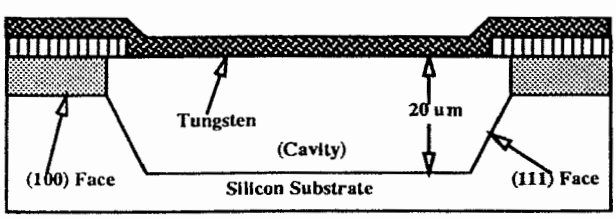

(c) After etching cavity in silicon substrate

Fig. 2 Process-flow cross sections

Tungsten has poor adhesion to Si_xN, so a thin (~0.1 μm) adhesion layer of Ti/W is first sputtered onto the wafer. A 0.7-μm film of LPCVD tungsten is then deposited, masked, and etched in an SF_6 plasma, leaving behind the tungsten filaments and contact pads. The tungsten-deposition conditions are designed to yield a low-tensile residual stress.

A timed etch in 10:1 HF removes the PSG in the Si_xN window underneath the tungsten filaments (while undercutting the Si_xN by a few micrometers), leaving them suspended over the silicon substrate (Fig. 2b). This allows the etchant in the next step to access the entire windowed silicon surface.

Finally, the cavity in the silicon substrate is anisotropically etched in a 100°C ethylenediamine pyrocatechol solution (EDP), which preferentially etches {111} crystal faces much more slowly than those in other directions (EDP, like 10:1 HF, does not attack tungsten). In contrast to etching isotropically, this step avoids undercutting of the Si_xN window and results in cavity walls that angle downward as shown in Fig. 2c. If the etch were continued long enough, a V-shaped groove would be formed, but in this process the etch is stopped when the cavity is about 20 μm deep.

Experimental Results: Microlamp

The microlamps discussed in this section have filaments with dimensions of 200 × 15 × ~0.7 μm. They have been powered by a range of dc voltages (V_{fil}), and their currents (I_{fil}) recorded. Plots of heating power (P_{fil}) and filament resistance (R_{fil}) vs. V_{fil} are shown in Fig. 3a.

The temperature of the filament (near its center) as a function of the heating power was measured with an optical pyrometer attached to a microscope. Because the microscope lenses absorb some of the radiation at the red wavelength to which the pyrometer is sensitive, the measured temperature values needed to be corrected (they were also corrected for the emissivity of the tungsten). The microlamp temperature vs. heating power, correct to within ±30 K, is shown in Fig. 3b. Taking the constant-temperature hot area to be 3000 μm², the efficiency of conversion of electrical energy to calculated radiative energy (integrated over all wavelengths) is plotted versus P_{fil} in Fig. 3c. While the efficiency increases with temperature, most of the input power is conducted away as heat, even at the highest filament temperatures. The calculated luminosity (using Planck's law, the emissivity as a function of temperature and wavelength, and the photopic response of the human eye) is about 5 millilumens for an input power of 120 mW. Even at moderate temperatures, the microlamp is easily visible to the naked eye at a distance of several meters.

Microlamp filament lifetime vs. temperature (for lifetimes shorter than about one hour) is plotted in Fig. 3d. Failure always occurs near the center of the filament due to material loss, apparently as a result of tungsten evaporation. Evidence for this evaporation is the specular material we observe to be deposited on the silicon substrate after the filament has burned out.

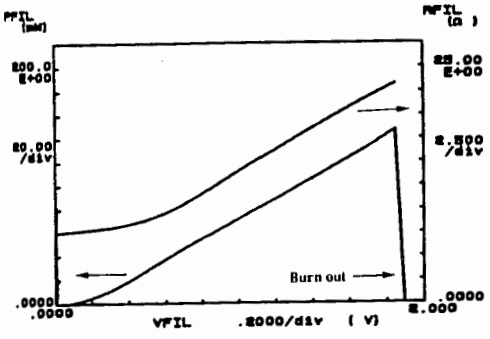

(a) Filament power and resistance vs. voltage

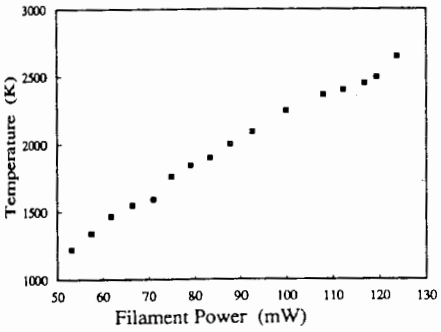

(b) Temperature vs. heating power

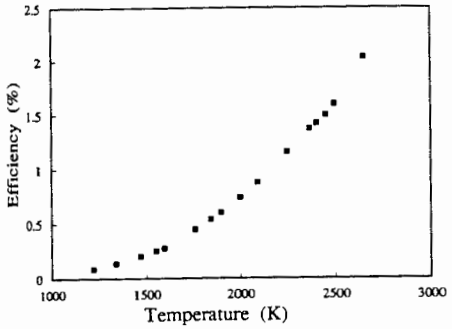

Efficiency of electrical to radiative power conversion vs. temperature

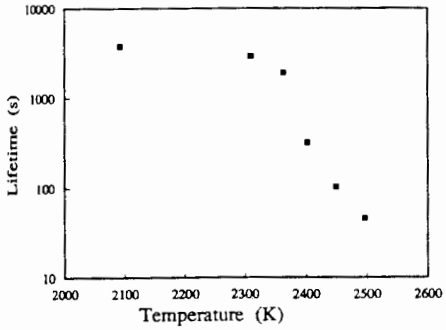

(d) Lifetime vs. temperature

Fig. 3 Microlamp

Experimental Results: Vacuum Microdiode

A circuit schematic for vacuum-microdiode operation is shown in Fig. 4a. Figure 4b, which is a plot of anode current I_A vs. anode voltage V_A at two different cathode temperatures, demonstrates three characteristic regions of operation: reverse bias, a space-charge-limited region, and a temperature-limited region.

Under reverse bias, no current flows because the cold anode cannot emit electrons. Under forward bias at low voltages, the current is limited by the space charge between the filaments and therefore depends only on V_A, independent of temperature. As the anode voltage is increased, the current becomes limited by thermionic emission from the cathode, which increases with cathode temperature. Current continues to increase with V_A because of Schottky-barrier lowering at the cathode surface [4].

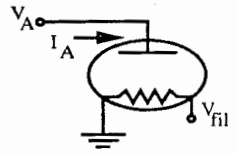

(a) Schematic

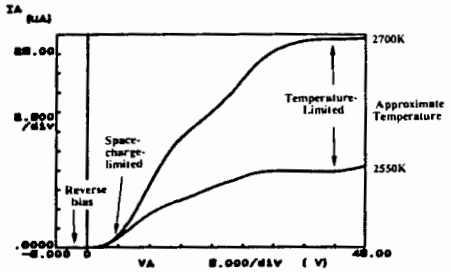

(b) Anode current vs. anode voltage at two temperatures

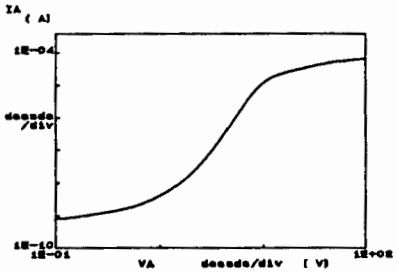

(c) log - log anode current vs. anode voltage

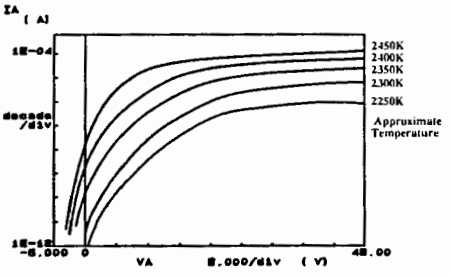

(d) log - linear anode current vs. anode voltage at several temps.

Fig. 4 Vacuum diode

According to fundamental vacuum-tube theory, the space-charge-limited current depends on voltage as

$$I_A = GV_A^{3/2} \quad , \tag{1}$$

where G is a constant for a fixed tube geometry known as the perveance [4]. A plot of log I_A vs. log V_A would, from (1), have a slope of 3/2, which does not match the measured microtube data (Fig. 4c). Over the two-decade V_A range of 0.1 to 100 V, the slope varies from 0.24 at low voltages to 4.6 at its steepest. We believe that this behavior results from a combination of effects including: *(i)* Schottky-barrier lowering; *(ii)* the nonconstant potential drop $[V_A - V_K(y)]$ (where $V_K(y)$ is the potential at a position y along the filamentary cathode length; V_K = 0 V at one end and V_{fil} at the other); *(iii)* the nonzero initial velocity of electrons leaving the cathode; and *(iv)* electrostatic deflection of the cathode when large electric fields are applied. These effects are generally not noticeable in macroscopic vacuum tubes.

The effect of an initial electron velocity is more apparent in the data of Fig. 4d, which shows curves of log I_A vs. V_A at several different filament temperatures. Under high anode bias, larger currents are measured at higher temperatures, as expected from the previous discussion. At zero and even small *negative* biases, however, *positive* currents are detected, because some of the electrons are thermionically emitted toward the anode with sufficient energy to travel against the applied electric field to reach the anode.

Experimental Results: Vacuum Microtriode

A circuit schematic for operation of microtriodes is shown in Fig. 5a. Figure 5b is a plot of anode current vs. anode voltage for a typical triode as the grid voltage V_G is stepped from zero to more negative voltages. The small-signal transconductance $g_m = \partial I_A/\partial V_G$ varies with operating point. A typical value, calculated from Fig. 5b at V_A = 10 V and V_G = 0 V, is –0.65 μS. The small-signal output resistance $r_o = \partial I_A/\partial V_A$ at this point is 3.0 MΩ.

The ratio of the effects of V_G and V_A on I_A is referred to as the amplification factor μ, where

$$\mu = -\partial V_A/\partial V_G \,|_{I_A=constant} \quad . \tag{2}$$

While g_m and r_o vary with operating point, μ has been observed to be relatively independent of V_A and V_G, as expected from vacuum-triode theory [4]. The amplification factor varies with device layout (cathode to grid spacing, cathode to anode spacing, grid width, etc.), but is typically in the range $1.5 < \mu < 6$ for our devices. For the example above, $\mu = -g_m \cdot r_{out} = 2.0$

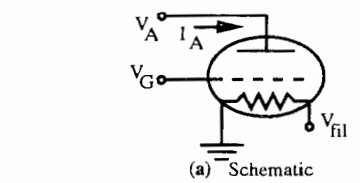

(a) Schematic

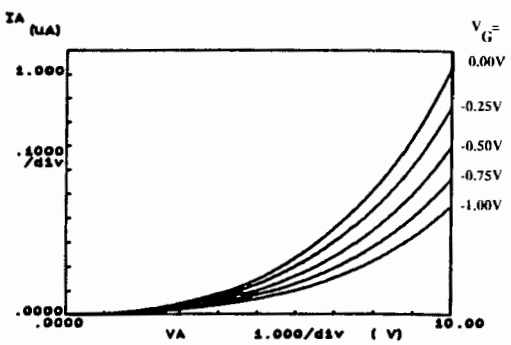

(b) Anode current vs. anode voltage at several gate voltages

Fig. 5 Vacuum triode

Conclusion

Hot-filament vacuum microdevices have been fabricated and tested as incandescent light sources and active circuit elements (microtubes). Microtubes fabricated thus far have short lifetimes due to evaporation of the hot tungsten filaments. Work-function-lowering coatings, such as those developed for conventional tubes, could be employed to reduce filament temperature and thereby lengthen the life of the microtubes. For the microlamps, which require high operating temperatures for high luminosity, evaporation can be slowed by operation in an inert gas.

Acknowledgments

We thank Simon Wong and Mark Beiley of the Center for Integrated Systems at Stanford University for the CVD tungsten deposition, and the staff of the U.C. Berkeley Microfabrication Laboratory.

References

[1] Takao Utsumi, "Vacuum microelectronics: What's new and exciting," (Keynote address of the Third International Vacuum Microelectronics Conference, Monterey, Calif.), IEEE Transactions on Electron Devices, vol. 38, no. 10 (Oct. 1990), pp. 2276-2283.

[2] S. Zurn, Q. Mei, C. Ye, T. Tamagawa, and D. L. Polla, "Sealed vacuum electronic devices by surface micromachining," *Technical Digest of 1991 International Electron Devices Meeting*, Washington, D.C., pp. 205-208, 1991.

[3] C. H. Mastrangelo and R. S. Muller, "Vacuum-sealed silicon micromachined incandescent light source," *Technical Digest of 1989 International Electron Devices Meeting*, Washington, D.C., pp. 503-506, 1989.

[4] Karl R. Spangenberg, *Vacuum Tubes*, McGraw-Hill, New York, 1948, pp. 46-48, 168-183.